SPONSOR

TiREX
EXPLORATIONS SHPK

SOME SURVEY AND INTERPRETATION PROBLEMS ON IP METHOD

Alfred Frashëri[1], Përparim Alikaj[1], Neki Frashëri[2]
Faculty of Geology and Mining ([1]) and Faculty of Informatics Technology ([2]), Polytechnic University of Tirana

Abstract

In the paper problems of IP mining exploration are analyzed and solutions presented. The dipole-dipole array configuration is considered as a symmetrical array in terms of the reciprocity principle. This paper demonstrates that the IP/Resistivity anomaly configurations depend on array geometry. The IP/Resistivity anomaly configuration observed with a C_1C_2 –P_1P_2 array is not the same as the one observed with a P_1P_2-C_1C_2 (reversed) array.

The inversion of IP pseudo-section of a dipole-dipole array survey is evaluated by resolution capability and stability of inversion solutions. The analysis presented in the paper, which is based on new data from mathematical and scale modeling of IP anomaly effect, as well as field survey results, presents also the necessity to taking into account aspects of non-linear IP phenomenon.

The analysis includes results of 2D and 3D mathematical and scale modeling performed in the Institute of Informatics and Applied Mathematics, and in the "Ligor Lubonja" Laboratory of Geophysics at the Faculty of Geology and Mining, Polytechnic University of Tirana and at the Geophysical Department, Albanian Geological Survey (Alikaj P. 1981, Frashëri A. et al. 1984, 1994, 1995, 2000).

Key words: Dipole-Dipole array, Reciprocity Principle, IP anomaly, Apparent Resistivity Anomaly, Inversion.

1. Introduction

In the practice of electrical prospecting surveys various array configurations are employed. The location of the current and potential electrodes is defined by the geological tasks to be solved. The dipole – dipole array is one of the most common arrays in mineral exploration. This is considered a symmetrical array in terms of the principle of reciprocity, so when the current

electrodes are respectively switched to potential electrodes the same responses in IP and resistivity values would be observed. However, our recent mathematical and scale models indicate discrepancies in this regard in several cases. This can lead to inaccurate target location and negative drilling results. To avoid such situations, the electrode orientation in the survey line has to be considered in the interpretation.

2. Presentation of the problem

The well-known reciprocity principle stands on the basis of many array configurations in electrical prospecting like pole - pole, dipole - dipole, Schlumberger, Wenner, etc. (Keller and Frischknecht 1966, Zabarovsky 1963, Frashëri et al. 1985). "According to the theorem of the reciprocity, no changes will be observed in the measured voltage if the placements of potential and current electrodes are interchanged. The reciprocity can readily be confirmed for an electrode array over a homogeneous earth" (Keller and Frischknecht 1966). Reciprocity principle has been discussed also by Parasnis D.S. (1988).

The heterogeneous medium presents a more complicated problem. Zabarovsky (1963) shows that if a body A has received an electrical charge Q_A, a body M will have a potential U_M related with the charge Q_A according to following the equation:

$$U_M = \alpha_{AM} \cdot Q_A$$

where α_{AM} is a coefficient dependant on the shape of bodies A and M, their reciprocal position and the boundaries of heterogeneity. If the reversed operation would take place, i.e. the body M to receive electrical charges of Q_M then the potential U_A of the body A would be:

$$U_A = \alpha_{MA} \cdot Q_M$$

In the electrostatic phenomena science it is proved that $\alpha_{AM} = \alpha_{MA}$. If this equality is true, then $Q_M=Q_A$ and as a consequence $U_M=U_A$. Translating this result into language of electrodynamics, one may say that the potential of electrode M created by the effect of electrode A would be equal to the potential of the electrode A, if the currents would be emitted in the ground by the electrode M, with the condition that the product $I * \rho$ remains the same. On this basis Zabarovsky (1963) concluded that the principle of reciprocity is valid for heterogeneous media as well. In homogeneous or horizontally stratified media the principle of reciprocity is true for any surveying array. In a heterogeneous environment this principle is absolutely true for four electrode Schlumberger, Wenner and pole-pole (half-Wenner) arrays. The dipole-dipole array presents a complex behaviour: for vertical targets of thickness $d > a$ (a stands for dipole spacing) the principle of reciprocity is met while for d comparable and thinner than a, the asymmetry is noticed in intensity and shape of the twin responses (Keller and Frischknecht 1966, Frasheri et al 1985). In IP method the principle of reciprocity is more complicated.

In several field surveys asymmetrical IP/Resistivity responses are observed with dipole – dipole array for opposite orientations of the potential and current electrodes in the survey line. To further investigate this phenomenon some mathematical models were carried out with a program of finite element method (Frasheri A. and Frasheri N. 2000).

In routine practice of electrical prospecting using dipole-dipole array little attention is paid to the evaluation of anomaly configuration regarding to position of target relative to current and

receiving electrodes. In many publications with the results of forward modeling and inversion, the position of electrodes in the survey line is not shown (Dey, A., and Morrison, H. F., 1979, Tsourlos, P.I., et al., 1998, Tsourlos, P. I. and Ogilvy, R. D. 1999). In certain conditions, this fact affects the results of target interpretation.

The mathematical computation of the IP effect is based on the Bleil 1953 and Seigel 1959 formulae:

$$U_{IP} = c \cdot \int_V \nabla U \cdot \left(\frac{1}{\vec{R}} \right) \cdot dv \qquad (1)$$

Where: U_{ip} is the IP potential;

$\vec{R}$ is the distance vector from the integration point to the receiving point;

∇U is the potential gradient of the primary electrical field, calculated by solving the finite element model.

To perform the mathematical modeling and the inversion of IP data, we have used the Komarov's (1972) approach:

$$C.(Uo+Uip) \approx C.Uo \qquad (2)$$

where: Uo is the potential of the primary electrical field,
Uip is the potential of the secondary electrical (IP) field,
C is the IP susceptibility.

Based on mathematical modeling of the IP anomalous field, there is a formal similarity of the polarizable medium and the increase of electrical specific resistivity of this medium as proposed by Komarov (1972) and used by many other authors (Avdeevic and Fokin 1992, Frasheri 1989, Frashëri et al 1994, Frashëri, and Frashëri 2000, Hmelevskoj and Shevshin 1994, Tsourlos , Szymanski and Tsokas, 1998, Tsourlos and Ogilvy, 1999):

$$\gamma^* = \gamma(1\text{-}m) \quad \text{or} \quad \rho^* = \frac{1}{\gamma(1-m)}; \qquad (3)$$

where: γ^*, ρ^* are fictive electrical conductivity and resistivity, considering the polarizability as well,

γ is electrical conductivity

m is IP chargeability

For 3D modeling of IP effect from targets with massive texture in homogeneous medium we have transformed the Bleil formulae, using Green's formulae (Frashëri N. 1983, Frashëri A., Frashëri N. 2000):

$$U_{IP} = c \cdot \int_S \left(\frac{1}{R} \right) \cdot \left(\frac{dU}{dn} \right) \cdot ds \qquad (4)$$

Where: R is the distance vector from the integration point to the measurement point
dU/dn is the gradient of the primary electrical potential on the boundary S of the target.

Fig.1 indicates the results of a mathematical IP model through finite element method, compared to a similar field situation. With the same method of finite elements, simultaneously with the IP effect, the apparent resistivity is calculated as well.

In Fig.2 are given the IP profiles obtained theoretically, calculated with our program and observed in scale model. In both figures it is noticed that the accuracy of mathematical model is good.

2. Numerical results for different models

Figs. 3 and 4 present the mathematical model results of IP and resistivity responses with dipole–dipole profiling. Two anomalies are observed on both parameters. Considering the reference plotting point in between the potential electrodes P_1 and P_2, one of the anomalies is obtained over the prism while the second one at a distance O_1O_2 , between the centers of the current and potential dipoles. This presentation is conditioned on the distribution of electrical field of the dipole - dipole array. Because a mirror image is missing in the center of the profiles, especially for IP, it means that $C_1C_2P_1P_2$ array responses are not equivalent with $P_1P_2C_1C_2$, or in mathematical terms, the principle of reciprocity is not strictly met. Keller (1966) presents the same phenomenon for the apparent resistivity.

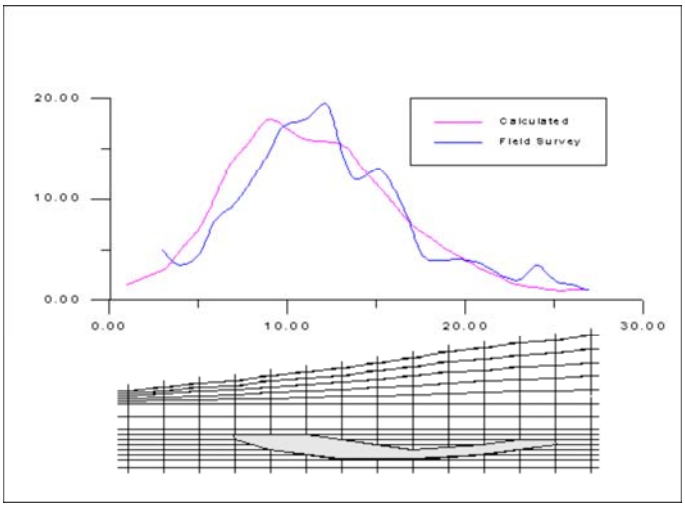

Fig. 1. A finite element section of an IP irregular body over a relief.

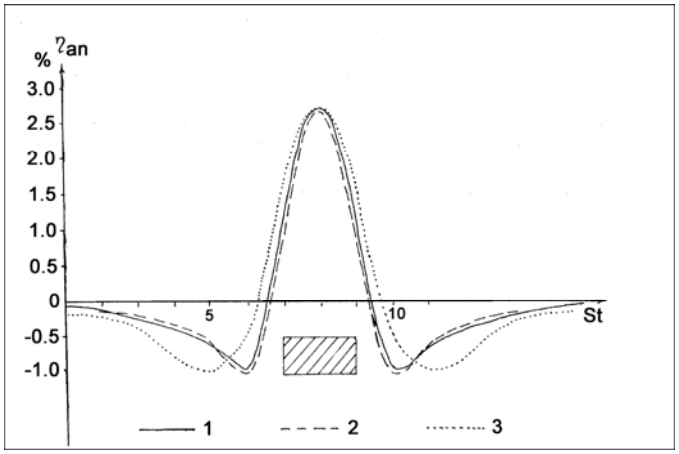

Fig. 2. IP profiling over a prism: Theoretical, calculated and physical modeling.

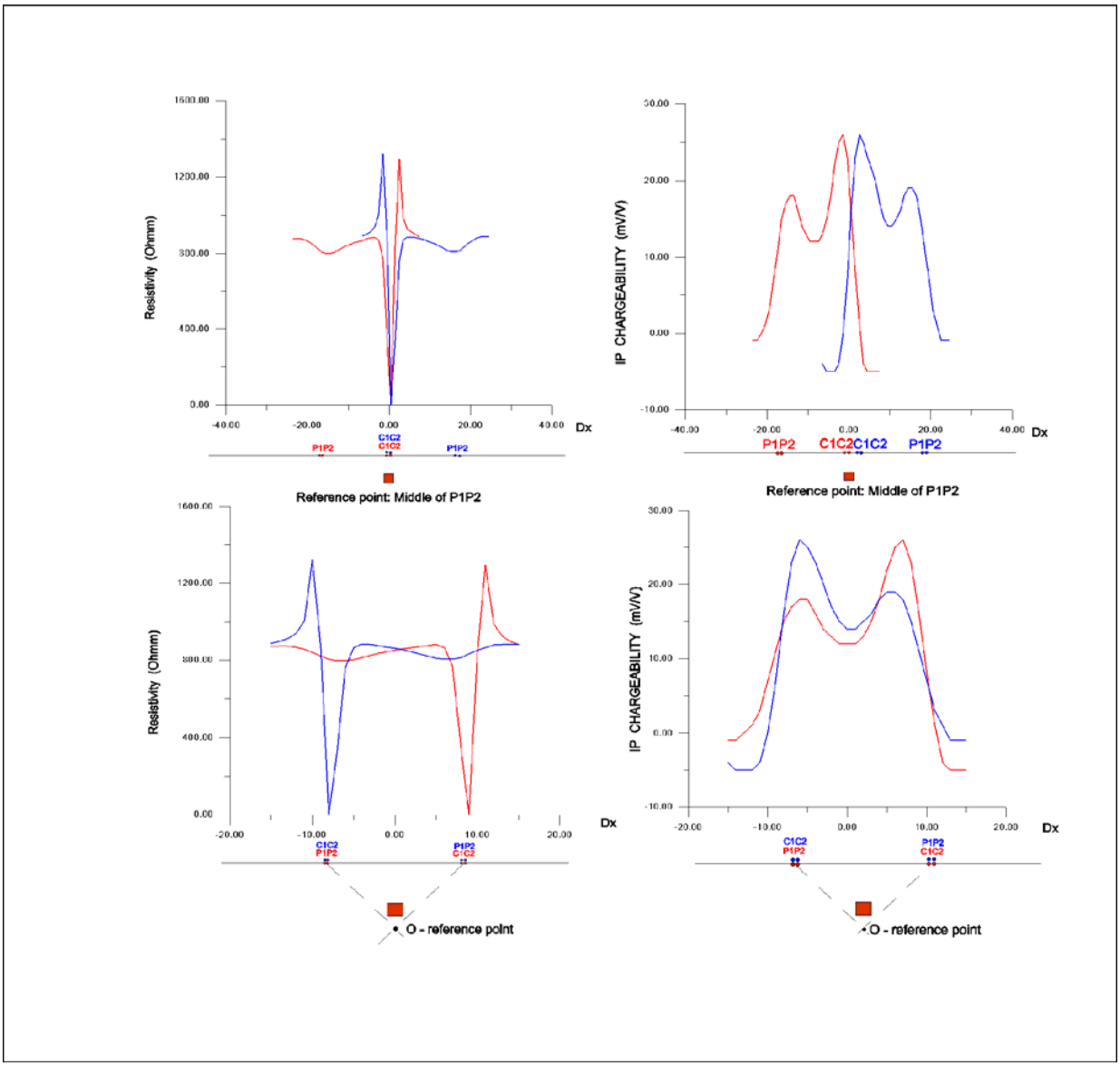

Fig. 3. IP and Resistivity mathematical modeling. Dipole-dipole profiling, C_1C_2-P_1P_2=1 Dx, n=16 Dx.
Model: 2D horizontal prism at depth 5 Dx, dimensions of the prism section 2 x 2 Dx. Resistivity of the prism 1 Ohmm, IP Chargeability 500 mV/V, Resistivity of the environment 1,000 Ohmm, IP Chargeability of the environment 0.01 mV/V.

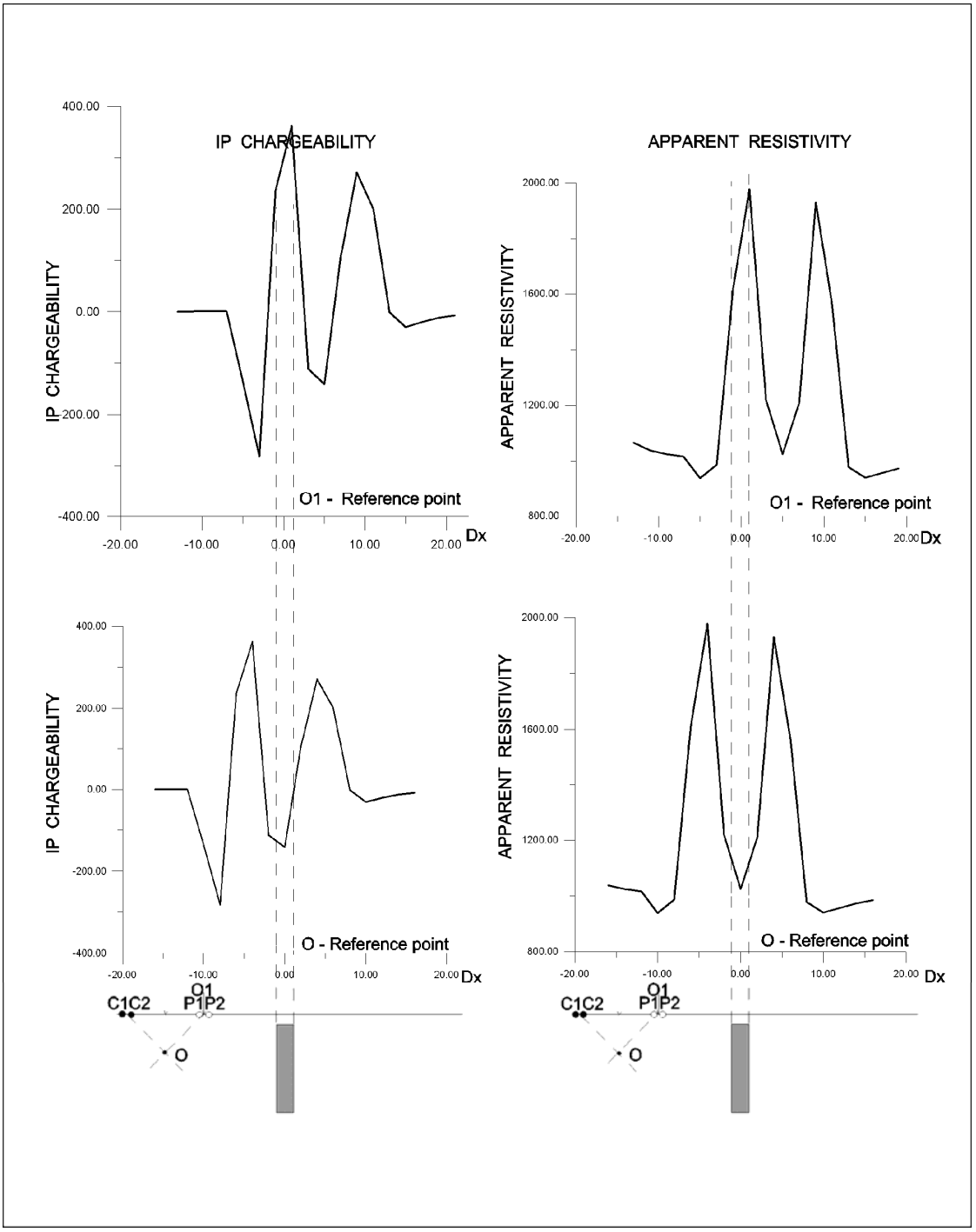

Fig. 4. IP and Resistivity mathematical modeling. Dipole-dipole profiling. C_1C_2-P1P2=2 Dx, n=1-10 Dx.

Model: 2D vertical prism at depth 1 Dx, dimensions of the prism section 2 x 9 Dx. Resistivity of the prism 20,000 Ohmm, IP Chargeability 500 mV/V, Resistivity of the environment 1,000 Ohmm, IP Chargeability of the environment 0.01 mV/V.

In pseudosection presentation, where the plotting point is located at the intersection of lines coming at 45° from midpoints between C_1C_2 and P_1P_2, these anomalies are located in both sides of the prism (Figs. 5, 6, 7, 8). For the resistivity parameter this location is almost symmetrical in shape and amplitude, for the vertical target (Fig. 5). The symmetry is perfect in cases when the thickness of the prism is equal or greater than the dipole spacing "a", and becomes poor for thinner prisms (Fig. 8).

Alternatively, the IP anomalies are asymmetrical even in cases of vertical prisms (Fig. 3, 5 and 8). In such cases, the epicentre of the most intensive anomaly is displaced on the side of current dipole C_1C_2. For shallow inclined prisms, the epicentres of both IP and resistivity anomalies are displaced on the opposite side of the dip.

The configuration of the IP/Resistivity anomaly is also dependent on the dip angle amplitude, relative to the current electrodes location.

The substantial difference between the electric field distributions in both cases clearly expresses the changes in IP anomaly configurations for gradient and dipole-dipole arrays. Fig. 9 depicts such variations. The amplitude and the asymmetry of IP anomaly depend on the orientation of the polarizing vector of the primary electric field in connection to the prism location. In fig. 10 is presented the electric polarizing field distribution for the gradient array and dipole-dipole array.

The response becomes more complicated when several targets are located under the surveying line. For a situation with two parallel polarisable inclined prisms like that in fig. 11, both C_1C_2-P_1P_2 and P_2P_1-C_2C_1 dipole-dipole arrays obtain a single IP anomaly in the centre and present some differences in contours shape. A formal interpretation or even an inversion on these results cannot outline the presence of two distinct targets. Our mathematical model with IP "Real Section" array (Alikaj 1981, Langore Alikaj and Gjovreku 1989, Lubonja, Frashëri and Alikaj 1994) over the same targets, however, provides a different picture with two distinct anomalies (Fig. 12).

In parallel with mathematical modelling, the asymmetrical configuration of the IP and resistivity anomalies depending on location of current and potential dipoles in relation to polarisable target is also supported by the scale modeling (Fig. 13).

Asymmetrical IP and resistivity anomalies, depending on the location of current and potential dipoles in relation to target is not always without problems in manual or inversion interpretations of the IP/Resistivity data surveyed with a dipole–dipole array.

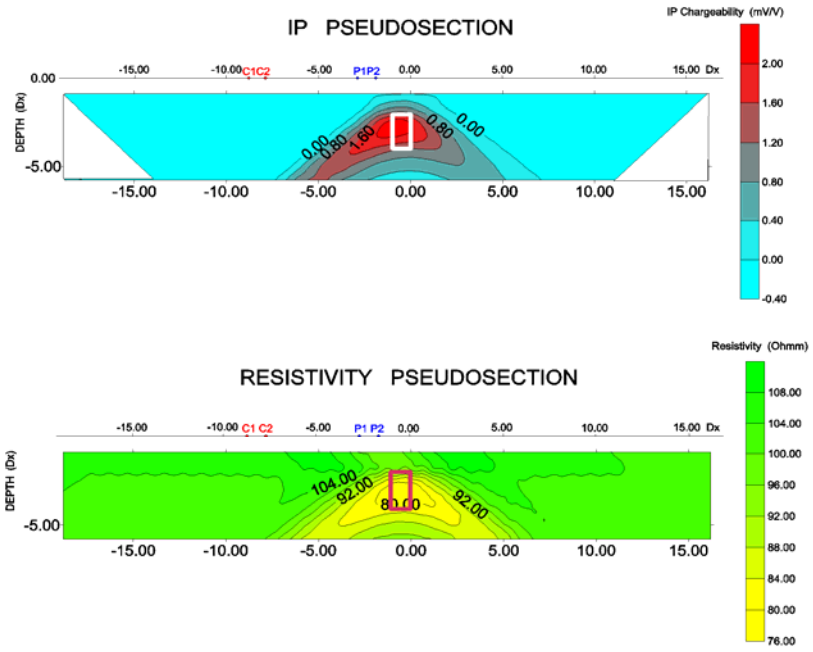

Fig. 5. IP and Resistivity Pseudosection with dipole-dipole array. C_1C_2-P_1P_2=1 Dx, n=1-11 Dx. Mathematical model: 2D vertical prism at depth 2 Dx, dimensions of the prism section 1 x 2 Dx. Resistivity of the prism 1 Ohmm, IP Chargeability 300 mV/V, Resistivity of the environment 100 Ohmm, IP Chargeability of the environment 0.01 mV/V.

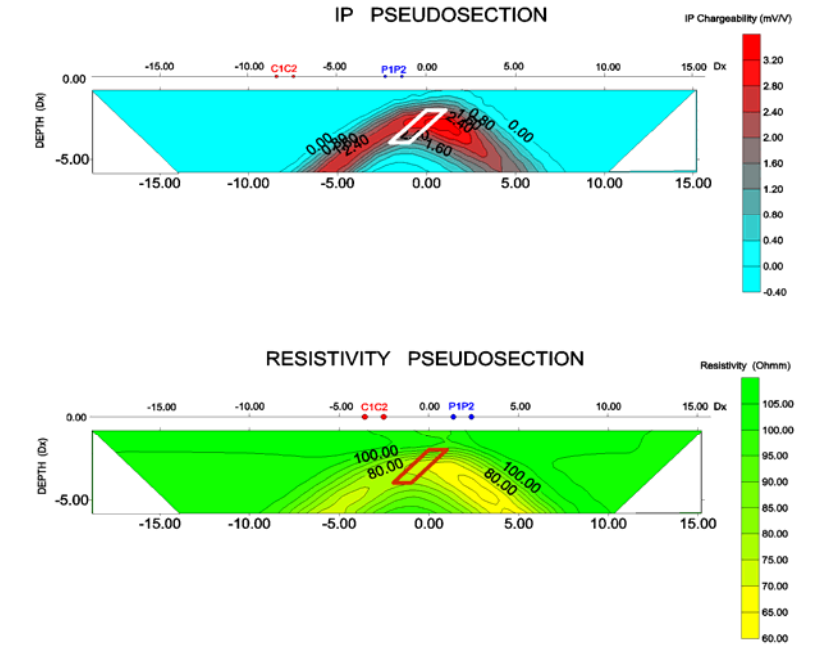

Fig. 6. IP and Resistivity Pseudosection with dipole-dipole array, C_1C_2-P_1P_2=1 Dx, n=1-11 Dx. Mathematical model: 2D inclined prism at depth 2 Dx, dimensions of the prism section 1 x 2 Dx. Resistivity of the prism 1 Ohmm, IP Chargeability 300 mV/V, Resistivity of the environment 100 Ohmm, IP Chargeability of the environment 0.01 mV/V.

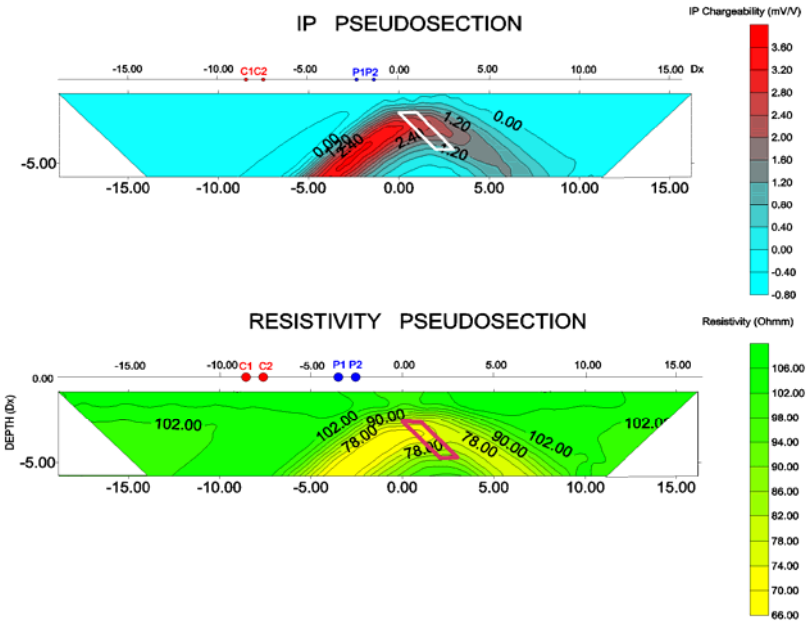

Fig. 7. IP and Resistivity Pseudosection with dipole-dipole array, P_1P_2-C_1C_2=1 Dx, n=1-11 Dx. Mathematical model: 2D inclined prism at depth 2 Dx, dimensions of the prism section 1 x 2 Dx. Resistivity of the prism 1 Ohmm, IP Chargeability 300 mV/V, Resistivity of the environment 100 Ohmm, IP Chargeability of the environment 0.01 mV/V.

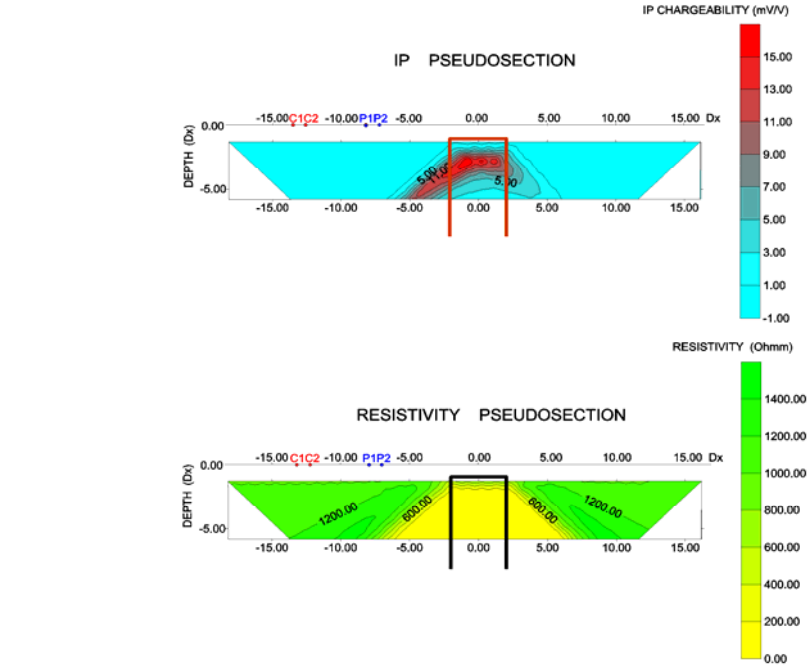

Fig. 8. IP and Resistivity Pseudosection with dipole-dipole array, C_1C_2-P_1P_2=1 Dx, n=1-11 Dx. Mathematical model: 2D vertical prism at depth 1 Dx, dimensions of the prism section 4 x 50 Dx. Resistivity of the prism 3 Ohmm, IP Chargeability 50 mV/V, Resistivity of the environment 1,000 Ohmm, IP Chargeability of the environment 0.01 mV/V.

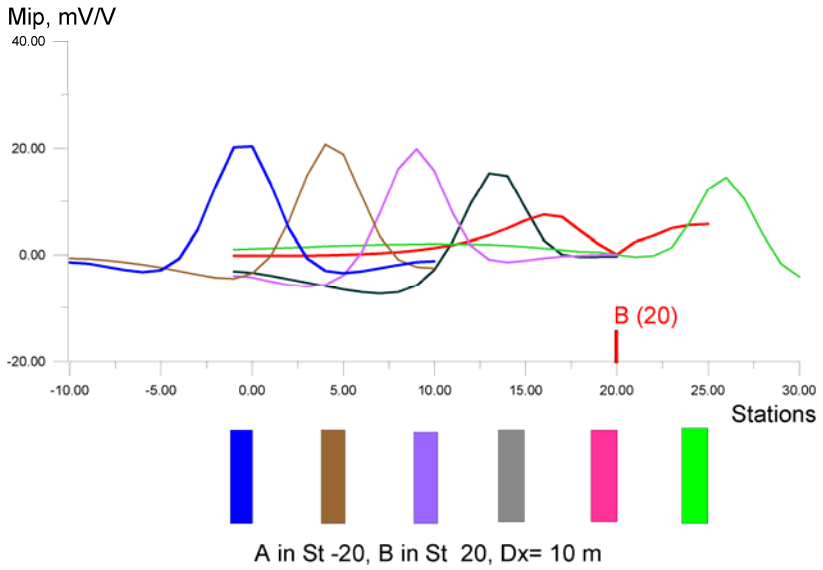

Fig. 9. IP anomaly configuration dependence on location of the target.

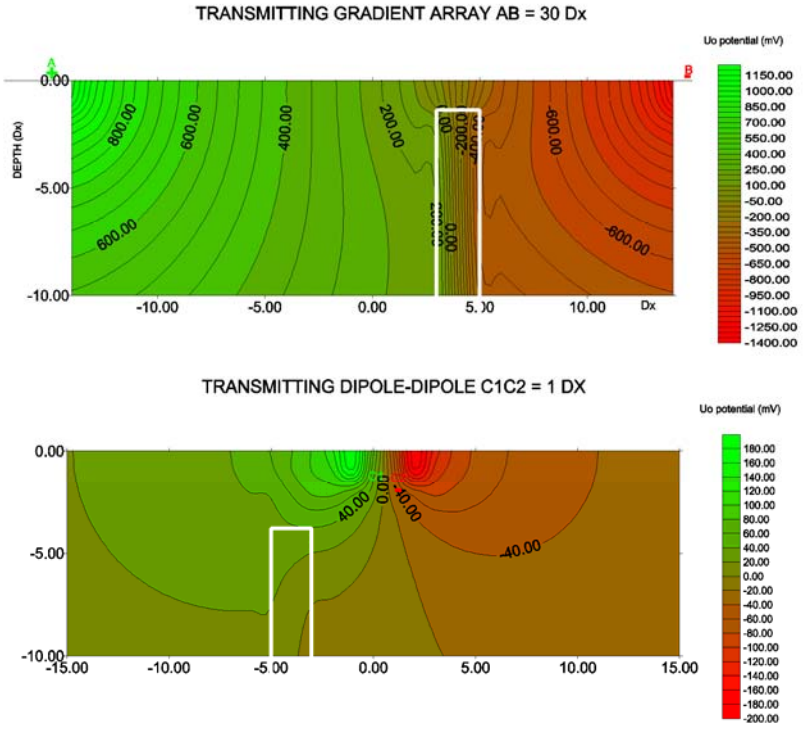

Fig. 10. Distribution of the primary electric field potential (Uo) of a transmitting dipole:
(a) Gradient array AB_{max} = 30 Dx
(b) Dipole-dipole array C_1C_2 = 1 Dx.
Mathematical model: Vertical prism. Dimensions of the prism 2 x 30 x 20 Dx, Resistivity of the prism 20,000 Ohmm, Resistivity of the environment 1,000 Ohmm.

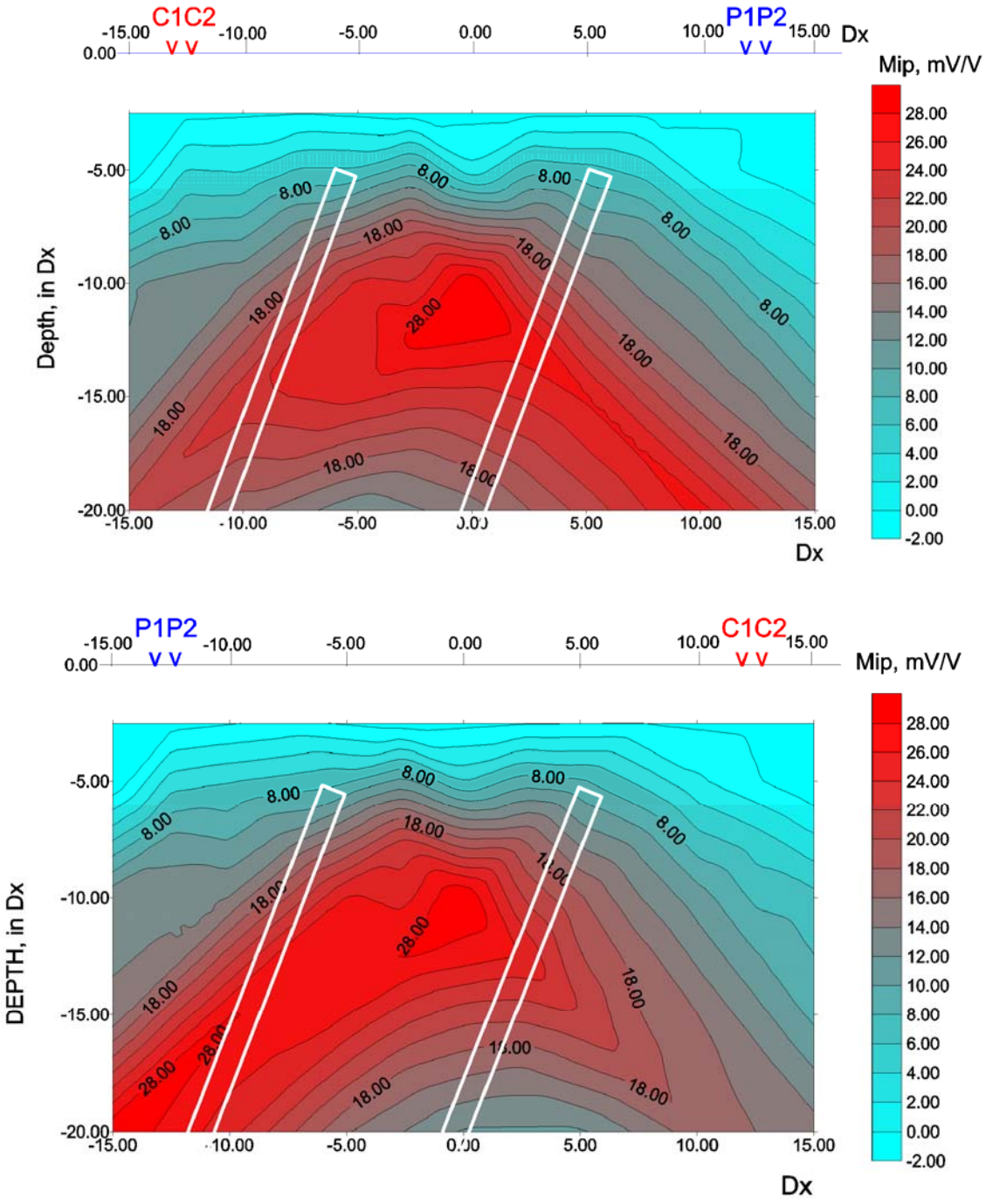

Fig. 11. IP Pseudosection with dipole-dipole array, $C_1C_2=P_1P_2=1$ Dx, n=1-39.
Mathematical Model: Two parallel inclined prisms (dip=70^o) at depth 5 Dx, dimensions of the prisms 1 x 20 x 20 Dx. Distance between the prisms 10 Dx, Resistivity of prisms 2000 Ohmm, IP Chargeability 500 mV/V, Environment Resistivity 500 Ohmm , IP Chargeability 0.01 mV/V.

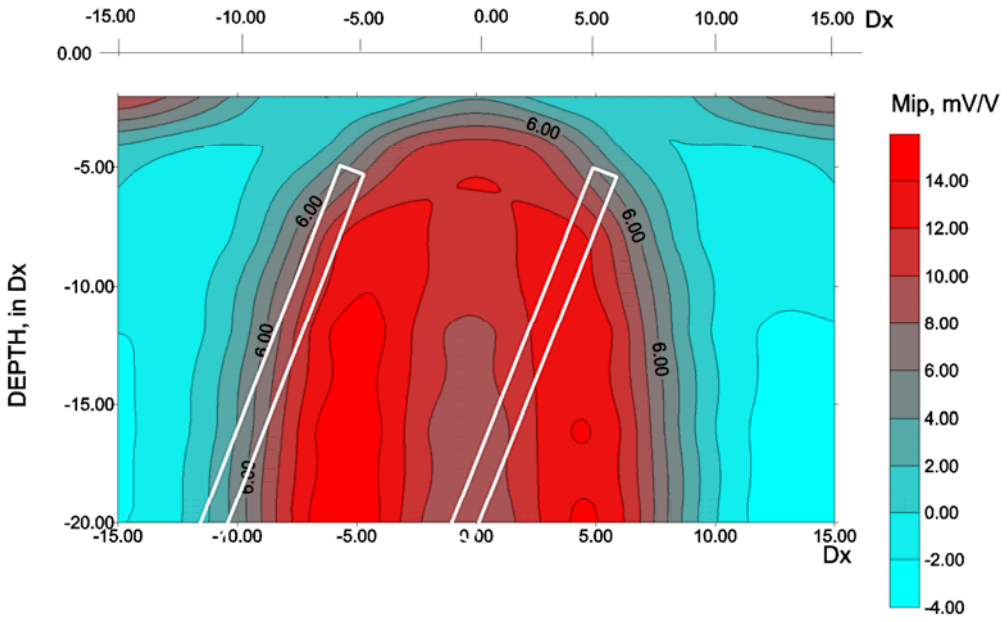

Fig. 12. IP "Real Section" with multiple gradient arrays. IP contour interval 2 mV/V.
Mathematical Model: Two parallel inclined prisms (dip=70^{o}) at depth 5 Dx, dimensions of the prisms 1 x 20 x 20 Dx. Distance between the prisms 10 Dx, Resistivity of prisms 2,000 Ohmm, IP Chargeability 500 mV/V, Environment Resistivity 500 Ohmm, IP Chargeability 1 mV/V.

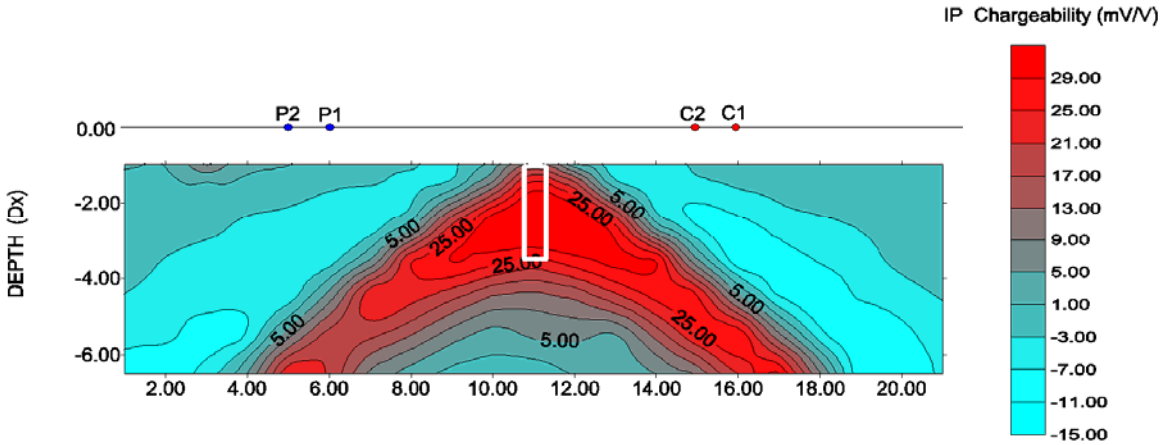

Fig. 13. IP Pseudosection with dipole-dipole array, $P_1P_2=C_1C_2=1$ Dx, n=1-24.
2D Scale Model: Target: Copper vertical prism at depth 1 Dx,
Section of the prism 0.5 x 2.5 Dx

3. Some considerations on IP data inversion

The inversion of IP data became a necessity to better define the attitude of a target in complex configuration of IP anomaly in section due to migration and array geometry.

In this part of the paper aspects of IP data inversion theory are considered, as well as resolution capability and stability of inversion solutions. This analysis is based also on new data from mathematical and physical modeling of abnormal IP effect, taking into account aspects of non-linear IP phenomenon.

The calculation of IP effect is based on the formula of Bleil. The evaluation of Komarov is used for both modeling and inversion of IP data, supposing a formal similarity of environment polarization with the increasing of its specific electrical resistivity. In all calculations, the effect of IP is supposed to be a linear phenomenon. Such modelling and inversions of IP pseudosections, carried out by many authors, have been steps forward for the interpretation of IP survey data and for the evaluation of IP method. But new facts on the non-linear nature of IP phenomenon, together with results of mathematical and physical modeling of last ten years rise new problems in IP modeling and inversion. If these problems will remain unsolved, the effectiveness of IP method will make no progress.

It is known that IP is considered as a linear phenomenon in all mathematical calculations, including inversion which creates several characteristics in the configuration of the mathematically calculated IP anomalies (Fig.5, 6, 7):

1. The upper part of anomaly corresponds with the upper edge of the polarized target.
2. Anomalies remain open towards the depth, even below the bottom edge of the targets.

Continuation of IP anomalies below bottom edge of targets makes the interpretation difficult and target extension determination at depth as unsure. The presentation of anomalies is more complex in pseudosections, for dipole-dipole survey configuration (Fig.5, 6, 7, 8, 10, 11). Migration of anomalies in pseudosections depends on dip angle of the targets and on position of transmitting and receiving dipoles relative to target (there are left-arrays C_1C_2-P_1P_2 and right-arrays P_1P_2-C_1C_2). The reason of such configuration of IP anomalies is due to assumption on linear behaviour of IP phenomenon in mathematical calculations, namely the primary and secondary voltages are linear in a broad band.

Due to the different polarizing situations, IP phenomenon is characterized by:

1. Near surface targets, due to surface polarization (massive sulphide) reach the nonlinearity regime of the secondary (IP) voltage very easily, because a major part of current density is attracted by them. As a result, the secondary voltage is grown faster than the primary voltage and consequently, their ratio (chargeability) reflects higher values.
2. Increasing the current dipole spacing in order to increase the depth of investigation, significant decrease of the primary (polarizing) voltage will take place at depth (Fig.10). Due to decreased current density, the secondary (IP) voltage will bear at its linear behaviour (proportional to primary voltage) and as a result a smaller chargeability anomaly will be obtained at depth. In Fig. 14 is presented an IP “Real Section” obtained in 2D scale model for a limited copper model at depth. As can be noticed, the IP contours outline a stronger

anomaly near the surface and they pinch out below the model bottom part. This is a clear non-linear effect of the IP phenomenon obtained in physical models that cannot be replicated in mathematical ones.

Voltage of the polarizing electric field at the depth 50 meters, in the environment with resistivity 1,000 Ohmm.

Tab.1

Current Electrodes C1C2 spacing, [in meters]	Voltage of the polarizing electric field, [in mV/m]
100	33.960
500	53
1000	13
2000	3
3000	1,4

3. The distributed IP effect is defined by survey arrays. This distribution is symmetric for gradient array, but asymmetric for dipole-dipole and pole-d ipole arrays (Fig. 10), making a necessity the inversion of IP data.

In contrast, the resistivity anomalies indicate closed contours below the target.

The stability and uniqueness of IP inversion solutions depend also on application of a linear model for the IP phenomenon, but that is not quite true for the whole variation of applied polarizing voltage. As a result, the lower part of polarized targets is instable in IP inversions. It becomes more instable when several targets are situated close to each other or in cases of targets near contacts between environments of different chargeability and resistivity. The increase of depth of targets causes the increase in inversion solution instability and resolution capability.

4. IP/Resistivity" Real Section" - a solution

Due to different polarizing situations, IP phenomenon is markedly conditioned by the significant decrease of the polarizing voltage at depth. Increasing the investigation depth, different parts of the same target, as well as targets located at different depths, are found in different polarizing conditions. This fact is clearly expressed in a contradiction between observed geoelectrical sections and numerical linear IP models for mathematical inversions at any polarizing voltages. As a result, the lower part of polarized target is instable in IP inversions. It becomes more instable when several targets are situated near to each other or in cases of targets near contacts between environments of different polarization and resistivity (Fig. 11). The increase of target's depth is accompanied by increasing of the inversion stability and decreasing of its solution's capability. At present level of the inversion, only the top of target is relatively well - determined in inverted section. The bottom edge of model remains uncertain as a-priory. A little can be determined as regard to deep angle in a qualitative way. In inversion section can be obtained some qualitative information on shape of the polarisable body as well.

IP "Real Section" performed with multiple gradient arrays or Vertical Electrical Soundings is actually the most appropriate scientific technique in presentation of anomalous chargeability distribution at section (Figs.14-20) (Alikaj 1981, Alikaj and Gordon 1999, Langore, Alikaj and Gjovreku 1989, Lubonja, Frasheri and Alikaj 1994). In difference to pseudo-section there is no lateral migration on top of target IP anomaly. Here are excluded the cases of lateral influence of other polarisable objects (Fig. 12). The "Real Section" presentation being very close to reality provides also very accurate results in "Real Section" inversion which leads to accurate verifications in mining works or drillings over IP anomalies Fig. 15, 16a, 16b, 17, 18, 19). The IP "Real Section" technique (Langore, Alikaj & Gjovreku, 1989) in field

surveys as well as physical models (Alikaj 1981) indicate a discrepancy in some cases with mathematical models (Frashëri A. and Frashëri N 2000). These cases include shallow locations of massive sulphide ore bodies or models (Fig. 18) and as explained above, it is connected to non-linear behaviour of IP phenomenon.

To achieve the level of today's requirements in certainty of surveys with IP method it is an imperative duty to be well studied the nonlinear nature of IP phenomenon. This will allow to be built an appropriate mathematical apparatus with real situation on this natural phenomenon. Only in that case, the inversion can be more accurate, in levels that allow its instability and non-uniqueness in its solution.

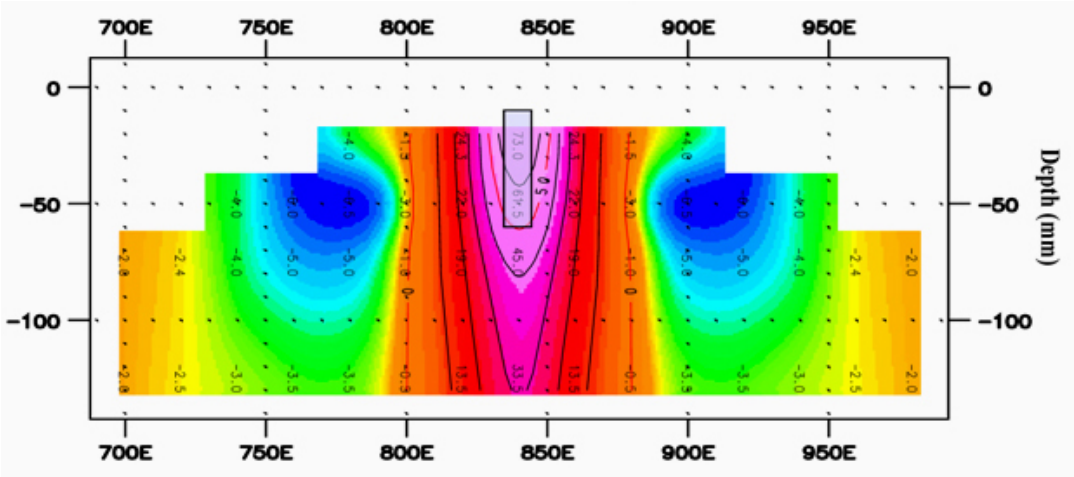

Fig. 14. Gradient "Real Section", 2D IP scale model. Array (MN=20 mm)

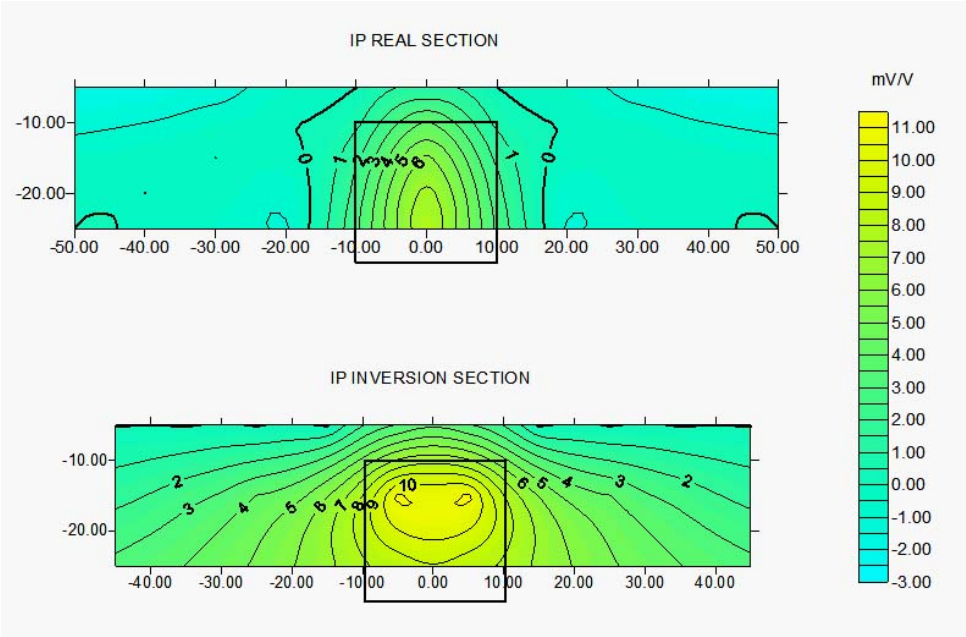

Fig. 15. IP "Real Section" and its Inversion Section.
2D Mathematical Model: Target: Prismatic Body, depth 10 m, height 20 m, width 20m, chargeability 200 mV/V.

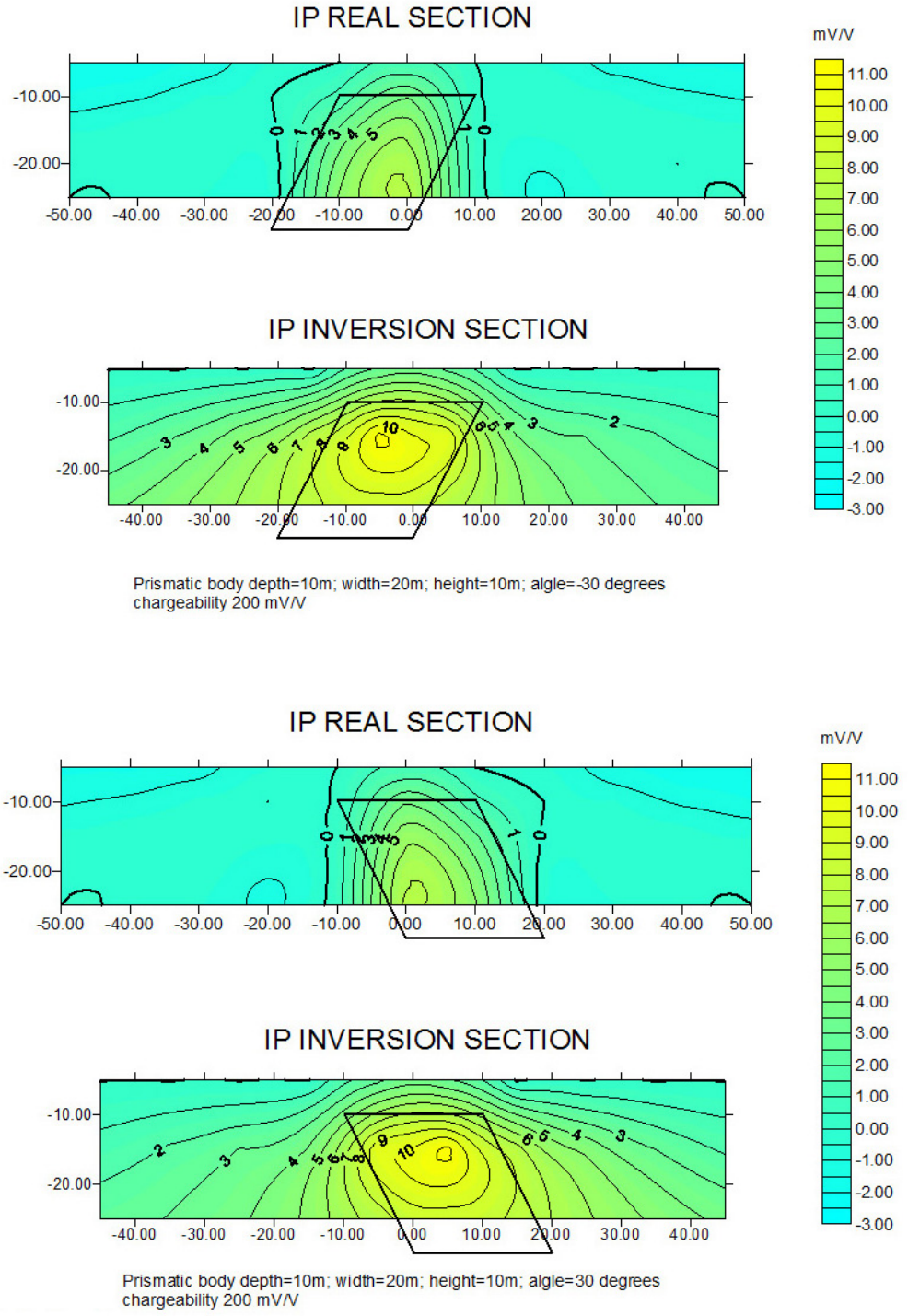

Fig. 16. IP "Real Section" and its Inverted Section.
2D Mathematical Model: Target: Prismatic Body, depth 10 m, height 20 m, width 20m, dip angle 60^{o}, dip azimuth 90^{o}, chargeability 200 mV/V.

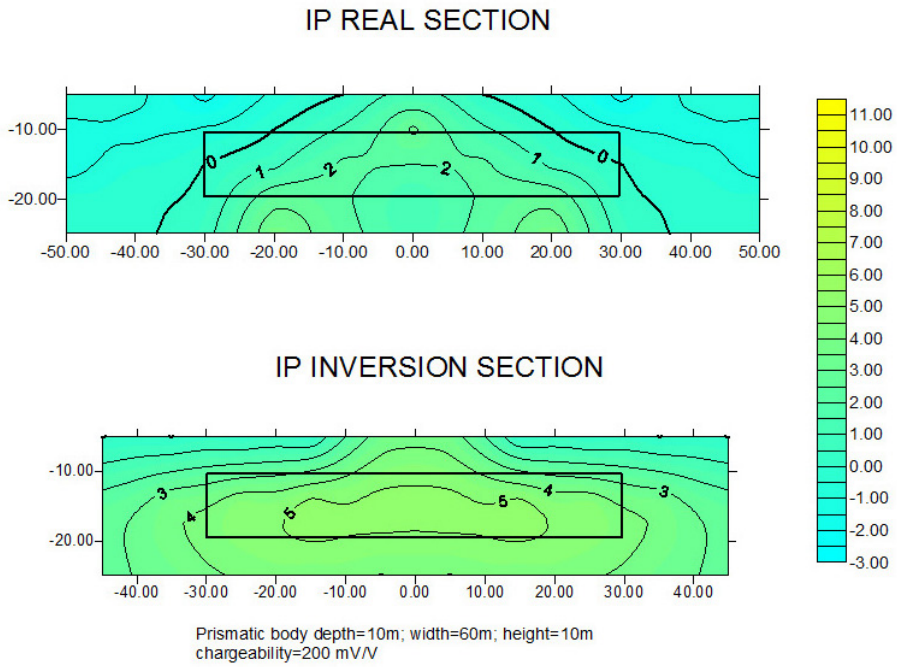

Fig. 17. IP "Real Section" and its Inverted Section.
2D Mathematical Model: Target: Horizontal Prismatic Body, depth 10 m, height 10 m, width 60m, chargeability 200 mV/V.

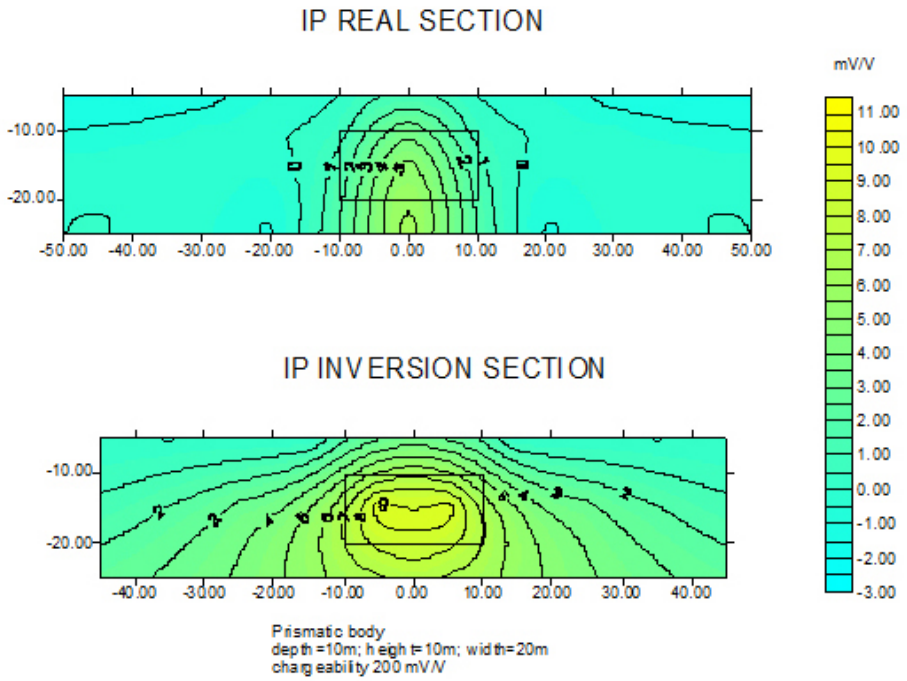

Fig. 18. IP "Real Section" and its Inverted Section. 2D Mathematical Model: Target: Horizontal Prismatic Body, depth 10 m, height 10 m, width 20m, chargeability 200 mV/V.

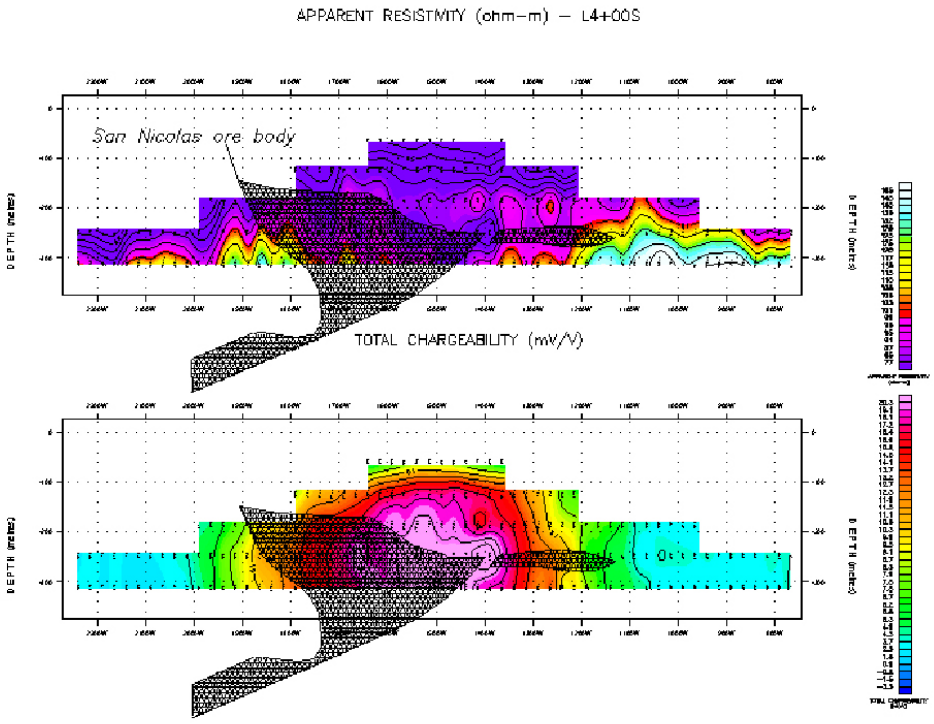

Fig. 19. Resistivity and IP "Real Sections" over San Nicolas polymetallic ore deposit, Mexico

Conclusions

1. The anomaly configuration in an IP/Resistivity survey with a dipole–dipole array is dependent on the location of the current and potential electrodes in connection to target. In this regard, logistical information about the survey should include the array orientation (left-array or right-array). The position of the array must be shown in plots and pseudo-sections. During the survey, it is necessary to keep the same orientation of current and receiving dipoles.

2. Physical modeling of IP shows the proof that there are differences between field survey cases and mathematical models. In sections compiled with data from physical models the anomalies are closed under the lower edge of the near surface target. In sections of mathematical linear models, the IP anomalies remain open at depth, contrary to those of apparent resistivity. This is due to the fact that in mathematical formulas the IP chargeability is considered as a linear phenomenon in the whole range of variation of polarizing voltage.

3. The use of mathematical formulas for inversion based on the linear IP phenomenon implies errors in compilation of sections based on approximation of inverted data. These errors may be comparable to instability of the inversion itself.

4. To achieve the levels of actual requirements for the quality of IP surveys, it is necessary to well evaluate the non-linear character of IP phenomenon. It would permit a better conception of mathematical basis of IP, as well as a better match with the real situation of the phenomenon in nature. Used with the IP inversion, these new mathematical non-linear equations would permit more exact results as compared to the instability and non-uniqueness of inversion solutions.

5. An accurate interpretation of IP/Resistivity data with dipole-dipole array should consider the information on electrode orientation on the survey line. The same recommendation is valid for the process of inversion interpretation.

6. The IP/Resistivity "Real Section" survey with multiple gradient arrays or series of Vertical Electrical Soundings provides a good corroboration between these electrical parameters and geological environment in section. The inversion of IP/Resistivity "Real Section" survey provides accurate results because the initial model provided by "Real Section" presentation is very close to reality.

References

Alikaj P., 1981. The physical modeling of IP "Real Sections" with different separations of gradient array. Albanian Geological Survey, Geophysical Department, Tirana, Albania.

Alikaj, P., 1994. A study on nonlinear spectral IP phenomenon. EAGE- 56th Meeting and Technical Exhibition - Vienna, Austria, 6-10 June 1994.

Alikaj P. and Gordon R. 1999. A geophysical tool for Mexican Geologic Environment. Presented at the Zacatecas Siglo XXI, Zacatecas, Mexico.

Avdeevic, M. M., Fokin A. F., 1992. Electrical Modeling of Geophysical Potential Fields. Publishing House Njedra, Sankt Peterburg, (in Russian).

Bleil D., 1953. Induced Polarization: a method for geophysical prospecting; Geophysics, 18, 636-662.

Dey, A., Morrison, H. F., 1979. Resistivity modeling for arbitrarily shaped three-dimensional structures. Geophysics, vol. 34, No. 4.

Frashëri A., Avxhiu R., Malaveci M., Alikaj P., Leci V., Gjovreku V. 1985. Electrical Prospecting. (In Albanian), Tirana University Publishing House. Tirana, Albania.

Frashëri, A., Tole, Dh., Frasheri, N., 1994. Finite element modeling of induced polarization electric potential field propagation caused by ore bodies of any geometrical shape, in mountainous relief. Commun. Fac. Sci., Univ. Ank. Serie C. V. 8, pp. 13-26 (1990).

Frashëri A., Lubonja L. Alikaj P. 1995. On the application of geophysics in the exploration for copper and chrome ores in Albania. Geophysical Prospecting 43, 743-757.

Frashëri, A., 1989. An algorithm for mathematical modeling of anomalous effect of Induced Polarization over rich copper ore bodies with any geometric shape. Bulletin of Geological Sciences (Tirana) No. 1, pp.116 - 126, (in Albanian, summary in English).

Frashëri A. Frasheri N. 2000. Finite element modeling of IP anomalous effect from ore bodies of any geometrical shape located in rugged relief area. Journal of Balkan Geophysical Society 1, 3-6

Frashëri, N., 1983. "Two Superparametric 4-node Elements to solve Elliptic Equations in Infinite Domains". Bulletin of Natural Sciences 1, 17-23. University of Tirana, (In Albanian, abstract in French).

Hmelevskoj V.K., Shevshin V.A., 1994. Elektrorazvjedka metodom soprotivlenia. Izdatelstvo Moskovskogo Universiteta, Moskva.

Keller G., V. and Frischknecht F. C., 1966. Electrical Methods in Geophysical Prospecting. Pergamon Press, Oxford, New York, Toronto, Sydney, Braunsckweig.

Komarov V.A. 1972. Electrical Prospecting for Induced Polarization Method. (In Russian). Published by Njedra.

Langore L., Alikaj P., and Gjovreku D. 1989. Achievements in copper exploration in Albania with IP and EM methods: Geophysical Prospecting 37, 975-991.

Lubonja, L., Frasheri, A., 1965. Induced Polarization method and its application for sulphide ore exploration. University of Tirana Publishing House (in Albanian).

Lubonja, L., Frasheri, A., Avxhiu, R., Duka, B., Alikaj, P., Bushati, S. 1985. Some trends in the increasing of the depth of geophysical investigation for ore deposits. Bulletin of Geological Sciences (Tirana) No. 3, pp. 33 - 52, (in Albanian, summary in English).

Parasnis D. S., 1988. Reciprocity Theorems in Geoelectric and Geoelectromagnetic Works. Geoexploration 25, 177-198, Elsevier Science Publishers B.V., Amsterdam, Printed in The Netherlands.

Seigel H.O. 1959. Mathematical formulation and type curves for Induced Polarization. Geophysics 37, 547-565.

Tsourlos, P.I., Szymanski, J.E., Tsokas G.N., 1998. Smoothness constrained algorithm for the fast 2-D inversion of DC resistivity and induced polarization data. Journal of Balkan Geophysical Society, Vol. 1, Numbers 1, pp 3-14.

Tsourlos, P.I., Ogilvy, R.D., 1999. An algorithm for the 3-D inversion of topographic resistivity and induced polarization data: Preliminary results. Journal of Balkan Geophysical Society, Vol. 2, Numbers 1, pp 30-46.

Zabarovskyy, A., I., 1963. Electrorazvyedka. Geoltehyzdat, Moscow.

Zienkiewicz, O., 1977. The Finite Element Method. McGraw Hill London.

LIST OF CAPTIONS

Fig. 1. A finite element section of an IP irregular body over a relief.

Fig. 2. IP profiling over a prism: Theoretical, calculated and physical modeling.

Fig. 3. IP and Resistivity mathematical modeling. Dipole-dipole profiling, C_1C_2-P_1P_2=1 Dx, n=16 Dx.
Model: 2D horizontal prism at depth 5 Dx, dimensions of the prism section 2 x 2 Dx. Resistivity of the prism 1 Ohmm, IP Chargeability 500 mV/V, Resistivity of the environment 1,000 Ohmm, IP Chargeability of the environment 0.01 mV/V.

Fig. 4. IP and Resistivity mathematical modeling. Dipole-dipole profiling. C_1C_2-P1P2=2 Dx, n=1-10 Dx.
Model: 2D vertical prism at depth 1 Dx, dimensions of the prism section 2 x 9 Dx. Resistivity of the prism 20,000 Ohmm, IP Chargeability 500 mV/V, Resistivity of the environment 1,000 Ohmm, IP Chargeability of the environment 0.01 mV/V.

Fig. 5. IP and Resistivity Pseudosection with dipole-dipole array. C_1C_2-P_1P_2=1 Dx, n=1-11 Dx.
Mathematical model: 2D vertical prism at depth 2 Dx, dimensions of the prism section

1 x 2 Dx. Resistivity of the prism 1 Ohmm, IP Chargeability 300 mV/V, Resistivity of the environment 100 Ohmm, IP Chargeability of the environment 0.01 mV/V.

Fig. 6. IP and Resistivity Pseudosection with dipole-dipole array, C_1C_2-P_1P_2=1 Dx, n=1-11 Dx.
Mathematical model: 2D inclined prism at depth 2 Dx, dimensions of the prism section 1 x 2 Dx. Resistivity of the prism 1 Ohmm, IP Chargeability 300 mV/V, Resistivity of the environment 100 Ohmm, IP Chargeability of the environment 0.01 mV/V.

Fig. 7. IP and Resistivity Pseudosection with dipole-dipole array, P_1P_2-$C_1C_{2=}$1 Dx, n=1-11 Dx.
Mathematical model: 2D inclined prism at depth 2 Dx, dimensions of the prism section 1 x 2 Dx. Resistivity of the prism 1 Ohmm, IP Chargeability 300 mV/V, Resistivity of the environment 100 Ohmm, IP Chargeability of the environment 0.01 mV/V.

Fig. 8. IP and Resistivity Pseudosection with dipole-dipole array, C_1C_2-P_1P_2=1 Dx, n=1-11 Dx.
Mathematical model: 2D vertical prism at depth 1 Dx, dimensions of the prism section 4 x 50 Dx. Resistivity of the prism 3 Ohmm, IP Chargeability 50 mV/V, Resistivity of the environment 1,000 Ohmm, IP Chargeability of the environment 0.01 mV/V.

Fig. 9. Distribution of the primary electric field potential (Uo) of a transmitting dipole:
(c) Gradient array AB_{max} = 30 Dx
(d) Dipole-dipole array C_1C_2 = 1 Dx.
Mathematical model: Vertical prism. Dimensions of the prism 2 x 30 x 20 Dx, Resistivity of the prism 20,000 Ohmm, Resistivity of the environment 1,000 Ohmm.

Fig. 10. IP anomaly configuration dependence on location of the target.
Mathematical model: Vertical prism.

Fig. 11. IP Pseudosection with dipole-dipole array, C_1C_2=P_1P_2=1 Dx, n=1-39.
Mathematical Model: Two parallel inclined prisms (dip=70^o) at depth 5 Dx, dimensions of the prisms 1 x 20 x 20 Dx. Distance between the prisms 10 Dx, Resistivity of prisms 2000 Ohmm, IP Chargeability 500 mV/V, Environment Resistivity 500 Ohmm , IP Chargeability 0.01 mV/V.

Fig. 12. IP "Real Section" with multiple gradient arrays.
IP contour interval 2 mV/V. Mathematical Model: Two parallel inclined prisms (dip=70^o) at depth 5 Dx, dimensions of the prisms 1 x 20 x 20 Dx. Distance between the prisms 10 Dx, Resistivity of prisms 2000 Ohmm, IP Chargeability 500 mV/V, Environment Resistivity 500 Ohmm, IP Chargeability 1 mV/V.

Fig. 13. IP Pseudosection with dipole-dipole array, P_1P_2=C_1C_2=1 Dx, n=1-24.
2D Scale Model: Target: Copper vertical prism at depth 1 Dx,
Section of the prism 0.5 x 2.5 Dx
Surrounding medium: fresh water

Fig. 14. 2D IP Chargeability scale model. Gradient "Real Section" Array (MN=20 mm)

Fig. 15. IP Real Section and its Inverted Section.
2D Mathematical Model: Target: Prismatic Body, depth 10 m, height 20 m, width 20m, chargeability 200 mV/V.

Fig. 16. IP "Real Section" and its Inverted Section.
2D Mathematical Model: Target: Prismatic Body, depth 10 m, height 20 m, width 20m, dip angle 60^o, chargeability 200 mV/V.

Fig. 17. IP "Real Section" and its Inverted Section.
2D Mathematical Model: Target: Prismatic Body, depth 10 m, height 10 m, width 60m, chargeability 200 mV/V.

Fig. 18. IP "Real Section" and its Inverted Section.

2D Scale Model: Target: Prismatic Body, depth 10 m, height 10 m, width 20m, chargeability 200 mV/V.

Fig. 19. IP/Resistivity “Real Section” over San Nicolas polymetallic ore deposit, Mexico.